Ultrasonics 95 (2019) 37–44

Contents lists available at ScienceDirect

Ultrasonics

journal homepage: www.elsevier.com/locate/ultras

Verification of the Kramers-Kronig relations between ultrasonic attenuation and phase velocity in a finite spectral range for CFRP composites

Yu.G. Sokolovskaya[a,*], N.B. Podymova[a], A.A. Karabutov[b,c]

[a] Faculty of Physics, M.V. Lomonosov Moscow State University, Leninskie Gory, Moscow 119991, Russia
[b] International Laser Center, M.V. Lomonosov Moscow State University, Leninskie Gory, Moscow 119991, Russia
[c] The National University of Science and Technology "MISiS", Leninskii Prospect 4, Moscow 119991, Russia

ARTICLE INFO

Keywords:
Kramers-Kronig relations
CFRP composites
Broadband laser-ultrasonic spectroscopy
Longitudinal acoustic waves
Phase velocity

ABSTRACT

The aim of this work is to verify applicability of the Kramers-Kronig relations between the attenuation coefficient and phase velocity of longitudinal acoustic waves in carbon fiber reinforced plastic (CFRP) composites in a finite megahertz frequency range. To measure these characteristics, the method of broadband acoustic spectroscopy with a laser source of ultrasound is used. We have experimentally shown that absolute attenuation in CFRPs is determined by both absorption in a polymer matrix and scattering on carbon fibers and gas pores of several tenths of microns in size. We have also found that the increasing composite porosity leads to the decrease in the absolute value of the ultrasonic velocity and to the increase in its relative dispersion in the entire studied frequency range of 1–10 MHz. The experimental results have shown that for the studied CFRPs in this range, features of the mechanism causing attenuation and dispersion of longitudinal acoustic waves by propagation in composites do not influence on applicability of the local Kramers-Kronig relations.

1. Introduction

It is well known that for electromagnetic and acoustic waves, the frequency dependences of the attenuation coefficient and phase velocity are connected by the general integral Kramers-Kronig relations, which are derived from the fundamental physical principles of causality and linearity [1–3]. The Kramers-Kronig integral relations are formulated in such a way that attenuation must be known at all frequencies in order to determine dispersion at each frequency, or vice versa [4]. For acoustic waves, these dispersion relations are written as integrals over the infinite frequency range, in which the real and imaginary parts of dynamic compressibility are as terms under integrals [3,5]. Therefore, the main difficulty in applying the general Kramers-Kronig relations directly to acoustic data is a limited bandwidth inherent in experimentally measured spectra of ultrasonic attenuation and the phase velocity. First of all, this bandwidth is determined by the operational parameters of the ultrasonic emitters and receivers such as a central frequency and effectively generated and detected frequency band, and also by a frequency transmission band for a medium under study, where ultrasonic parameters can be measured with sufficient accuracy. By restricting the integration domain to the measured spectrum, errors could occur that can seriously influence on the calculation results. Hence, from the scientific point of view it is interesting and worthwhile to analyze the applicability of the Kramers-Kronig relations in a limited acoustic frequency range (see, for example, [3,5,6]). The approximate relations called as local can be obtained for a limited frequency range from the general relations under condition of no resonances in acoustic attenuation and velocity dispersion in the studied frequency range [2,3,5]. Detailed explanation of why resonances are a fundamental restriction is given in Section 2 by deriving expression (6).

In general, attenuation of acoustic waves in a medium can be caused by absorption, scattering, beam divergence due to diffraction, or a combination of these mechanisms. The Kramers-Kronig relations should be fulfilled independent on a particular physical reason causing attenuation and dispersion of acoustic waves in a medium [3,5]. To verify validity of the Kramers-Kronig relations in a limited frequency range, the broadband acoustic spectroscopy method is appropriate (see, for example, [7]). This method makes it possible to study dynamic processes in materials occurring in the ultrasonic field, as well as to perform nondestructive evaluation of the internal structure of various condensed media [8–10]. In the past decades, an extremely large number of works especially devoted to the broadband acoustic spectroscopy of a variety of homogeneous viscoelastic materials were published (see, for example, [4,11–14] and references sited therein). But the detailed review of these studies is out of the frames of this work.

The natural resonance behavior of piezoelectric transducers of

* Corresponding author.
E-mail address: yu.sokolovskaya@mail.ru (Y.G. Sokolovskaya).

https://doi.org/10.1016/j.ultras.2019.03.004
Received 10 January 2019; Received in revised form 1 March 2019; Accepted 4 March 2019
Available online 05 March 2019
0041-624X/

ultrasound [15] causes certain engineering difficulties by broadband measurements of ultrasonic attenuation and velocity. As a rule, to perform ultrasonic measurements in a broad spectral range, a set of several piezoelectric transducers with various central frequencies is used (see, for example, [9,10,16]). The multiple rearrangement of transducers could introduce additional errors by time-of-flight measurements for waves propagating over the acoustic path and, correspondingly, by calculations of the phase shifts and phase velocity. This is true solely for the pitch-catch/through-transmission method, and in the pulse-echo method there is far less apparatus inconsistency and corresponding configuration unrepeatability. But in the last case, additional attenuation of an ultrasonic pulse during double-pass through a specimen occurs. Therefore, effective narrowing of the operating frequency bandwidth and corresponding extra measurement errors for high-frequency harmonics as compared with the through-transmission method are inherent in the pulse-echo method.

It should be noted that verification of the dispersion relations was previously performed mainly for liquids and gases. Probably, this is because of liquids and gases under study can serve itself as an acoustic immersion contact between an emitter and receiver. This allows one to measure ultrasonic parameters for such media with a sufficient accuracy.

Below, we review briefly the earliest and most representative works concerning verification of validity of the local Kramers-Kronig relations between ultrasonic attenuation and phase-velocity dispersion in substances of different nature (liquids, gases, solids, and biological tissues). In almost all these media, sound attenuation was mainly caused by absorption and practically no scattering was observed.

The authors of [3,17] have performed verification these relations in the human blood solutions of different concentrations. For this medium, ultrasonic absorption depends on concentrations of hemoglobin and albumin. To measure ultrasonic absorption and velocity dispersion in the spectral range of 1–10 MHz, a set of several barium titanate based piezoelectric transducers was used. Another study of biological tissues is described in [18], where the dispersion relations are considered for porcine ventricular myocardium in the range of 2.5–13 MHz. In both cases, the authors have confirmed applicability of the Kramers-Kronig relations in the studied frequency ranges.

The authors of [5,19] obtained the frequency dependences of absorption and velocity dispersion of ultrasound for the cobalt copperas solution and polyethylene in the range of 1–10 MHz using the technique similar to that described in [17]. Although different mechanisms of absorption of ultrasound exist in these media, it was confirmed that the approximate form of the Kramers-Kronig relations can be used to find the relationship between these ultrasonic parameters. Similar studies were performed in [16] for amorphous (PMMA) and polycrystalline (polyamide, polyethylene, polypropylene) polymers in the frequency range of 5–25 MHz. Here, also different interaction mechanisms of ultrasound with the internal structure of polymers cause absorption in amorphous and additional scattering in polycrystalline polymers, but also a good agreement between the theory and experimental results was obtained.

In addition to the aforementioned cases, the experimental studies of the dispersion relations were performed for a number of organic liquids, such as castor- and carbon-based oils, and for gelatin-based phantoms with different concentrations of graphite particles [20,21]. It has been shown that for oils, the Kramers-Kronig relations are met in the range of 1.5–20 MHz, and for model phantoms in the range 1.2–6 MHz.

Similar studies were performed for air of different humidity [22]. Attenuation and the phase velocity of sound were measured in the range 100 Hz–1 MHz; the dispersion relations were satisfied up to 10 kHz, but for higher frequencies, discrepancy between the theory and experimental results was observed. Dependences of the sound velocity in air on its humidity, pressure, and temperature were mentioned as possible reasons of this discrepancy.

Especially, work [23] should be noted, the authors of which were probably the first to study the local Kramers-Kronig relations between the ultrasonic attenuation coefficient and phase velocity in CFRPs. In such material, two mechanisms of decay in the acoustic-wave energy are simultaneously realized, namely, absorption in a polymer matrix and scattering on carbon fibers. However, the authors presented the calculation results for the dispersion relations only for several discrete frequency points in the range from 3 to 8 MHz. In addition, to calculate dispersion of the ultrasonic velocity, not the experimental frequency dependences of the attenuation coefficient, but their linear approximations were used. Obviously, it reduces applicability of the Kramers-Kronig relations.

To solve the problem of reliable measurements of ultrasonic parameters in a wide frequency range, the application of laser ultrasonics [24,25] is very promising. The amplitude and temporal profile and consequently the acoustic frequency spectrum of an ultrasonic pulse thermally induced by absorption of a laser pulse are determined by a time profile of the laser intensity, and by the light absorption coefficient, volume thermal expansion coefficient, heat capacity, thermal conductivity, and acoustic boundary conditions at the surface of a medium, which serves as a source of ultrasound. By absorption of nanosecond pulses of a Q-switched laser with energy of several mJ, the amplitude of thermooptically induced ultrasonic pulses may reach several hundreds of MPa in a frequency range from hundreds of kHz to hundreds of MHz [26–29]. The setup for the broadband acoustic spectroscopy with a specially designed laser source of ultrasound (the so-called laser-ultrasonic spectroscopy) was firstly proposed and designed in [30] to study acoustic properties of heterogeneous colloid water solutions of bentonite clays in the frequency range of 1–50 MHz. Further, this technique was successfully used to analyze fatigue structural changes in glass-fiber-reinforced-plastics using the attenuation spectra of longitudinal ultrasonic waves [31] and to study the influence of structural defects like porosity and delaminations in CFRPs on the resonance attenuation features of longitudinal ultrasonic waves [32]. In our opinion, the main advantage of laser excitation of ultrasound as compared with piezoelectric excitation is the ratio of the highest and the lowest frequencies, f_{max}/f_{min} , of the spectral bandwidth of laser-induced ultrasonic pulses. This ratio can be 10–20 times higher than that for piezoelectric transducers. The ratio f_{max}/f_{min} for laser-induced ultrasonic pulses depends mainly on the laser-pulse duration and the light absorption coefficient of a source of ultrasound. For example, in the experimental setup described in [30] the ratio f_{max}/f_{min} was approximately 50. The additional advantages include the absence of ringing in a reference laser-induced ultrasonic pulse and its side-lobe free directivity pattern.

This work aims to experimentally verify applicability of the local Kramers-Kronig relations in CFRPs using the method of acoustic spectroscopy with a laser source of ultrasound and high-sensitivity piezoelectric detection of broadband acoustic pulses. Since CFRPs intensely absorb and scatter ultrasound in the megahertz range, this method is appropriate to carry out high-precision measurements of the frequency-dependent attenuation coefficient and phase velocity in this range. Using the experimentally measured ultrasonic attenuation coefficient in the frequency range of 1–10 MHz, we calculated the phase-velocity dispersion in the same range with an approximate local form of Kramers-Kronig relations and compared it with the experimentally obtained phase velocity. The main idea of our work was to demonstrate the possibility to apply the local Kramers-Kronig relations in the limited frequency range for materials, which not only effectively absorb but also scatter ultrasonic waves.

2. Formulation of the problem

For acoustic waves in an isotropic medium obeying the general Hook's law, the Kramers-Kronig relations for the real and imaginary parts of dynamic compressibility are written as

$$K_1(\omega) - K_1(\infty) = \frac{2}{\pi}\int_0^\infty \frac{\omega' K_2(\omega')}{\omega'^2 - \omega^2} d\omega',$$

$$K_2(\omega) = -\frac{2\omega}{\pi}\int_0^\infty \frac{K_1(\omega') - K_1(\infty)}{\omega'^2 - \omega^2} d\omega', \quad (1)$$

where $K = K_1 + iK_2$ is reciprocal to the bulk elastic modulus [33], $\omega = 2\pi f$, f is the frequency of an acoustic wave.

Using the known dispersion relation for acoustic waves

$$k^2 = \omega^2 \rho_0 K(\omega), \quad (2)$$

where k is the wave number, and taking into account that

$$k = \frac{\omega}{C(\omega)} + i\alpha(\omega) \quad (3)$$

the relations between compressibility, attenuation coefficient $\alpha(\omega)$, and phase velocity $C(\omega)$ are written as (see equations (14a) and (14b) in [5]):

$$\frac{\omega^2}{C^2(\omega)} - \alpha^2(\omega) = \omega^2 \rho_0 K_1(\omega),$$

$$\frac{2\alpha(\omega)}{C(\omega)} = \omega \rho_0 K_2(\omega). \quad (4)$$

For condition $\frac{\alpha(\omega)C(\omega)}{\omega} << 1$ called as the sound approximation and fulfilled in the megahertz frequency range (equations (15a) and (15b) in [5]):

$$C(\omega) = \frac{1}{\sqrt{\rho_0 K_1(\omega)}},$$

$$\alpha(\omega) = \frac{1}{2}\rho_0 C(\omega)\omega K_2(\omega). \quad (5)$$

Taking into account (1), expressions (5) describe the relation between attenuation and phase-velocity dispersion and of acoustic waves in the infinite frequency range. They could only be used when a major contribution to infinite integrals is strictly frequency-localized [5]. Actually, infinite limits of integration in (1) are "conditional", since the sound approximation is fulfilled only for wavelengths, which considerably exceed atomic spacing and for solids, calculations are only performed using expressions (5) up to frequencies of about 10^{14} Hz [2].

To make a comparison with experimental data obtained in a limited frequency range, we should go from the general Kramers-Kronig relations to its local form. In certain frequency range $[\omega_0,\ \omega]$, the approximate local relations could be derived, if in this range the frequency dependences of the ultrasonic attenuation coefficient and phase velocity are monotonic, i.e., have no local extremes and resonances [5]. In this case, the imaginary part of dynamic compressibility $K_2(\omega)$ in (1) could be expanded to series over frequency in the vicinity of ω_0, and terms in this series corresponding to derivatives of higher orders could be neglected [5]. Then, the relation between the imaginary part of compressibility and the local rate of change of its real part at the same frequency is written as

$$K_2(\omega) = -\frac{\pi}{2}\omega\frac{dK_1(\omega)}{d\omega}. \quad (6)$$

Using formulas (4) and (6), we obtain the local Kramers-Kronig relations in frequency range $[\omega_0,\ \omega]$:

$$\alpha(\omega) = \frac{\pi\omega^2}{2C_0^2}\frac{dC(\omega)}{d\omega} \quad (7)$$

$$C(\omega) = \left(\frac{1}{C_0} - \frac{2}{\pi}\int_{\omega_0}^{\omega}\frac{\alpha(\omega')}{\omega'^2}d\omega'\right)^{-1} \quad (8)$$

Hence, expressions (7) and (8) describe the relationship between the attenuation coefficient and phase velocity dispersion of longitudinal acoustic waves in given limited range $[\omega_0,\ \omega]$. By performing experiments, it corresponds to the operating frequency range where $\alpha(\omega)$ and $C(\omega)$ are measured. These expressions show the relation between $\alpha(\omega)$ and $C(\omega)$ without referring to their particular functional dependence on frequency, for instance, such as different power-law approximations for viscoelastic homogeneous polymers (see, for example [34] and references sited therein). Demonstration of the applicability of such particular approximations of acoustic characteristics for the CFRP composites, which contain only 30–50% of a viscoelastic matrix and the rest is the rigid carbon fibers with acoustic properties absolutely differing from that of viscoelastic polymers, is beyond the scope of this work.

3. Methodology and materials

3.1. Parameters of CFRP specimens

The specimens under study are epoxy-based uni-directional CFRP laminates cut as rectangular parallelepipeds with lateral dimensions 70 mm × 20 mm and thickness H = 10.4–12.4 mm. The diameter of a single carbon fiber is 5 μm and the mean thickness of each ply is 200 μm. For the ultrasonic spectroscopy procedure composite specimens are placed so that the reference ultrasonic pulse propagates in the plane of the specimen isotropy normal to the fiber plies.

The ultrasonic attenuation in CFRPs is caused by absorption in the epoxy matrix and scattering on carbon fibers. The matrix is an amorphous polymer, in which ultrasonic absorption occurs due to the transformation of the acoustic energy into the energy of vibrational and rotational modes of molecular chains. The frequency dependences of the attenuation coefficient and phase velocity of longitudinal acoustic waves are determined by energies of the intramolecular and intermolecular interaction, parameters of the relaxation processes, and by a pattern and intensity of molecular motions [35]. Peculiarities of the intermolecular interaction in the presence of long molecular chains lead to occurrence of a spectrum of relaxation times, which in turn leads to occurrence of related frequency-dependent ultrasonic attenuation and phase-velocity dispersion.

Along with scattering of acoustic waves on carbon fibers, additional scattering could occur in CFRPs caused by small gas pores in the material. These pores are typically 10–50 μm in size, which was determined with the X-ray computer tomography. The representative X-ray image of a cross-section of one of the studied specimens showing an irregular distribution of pores within epoxy layers is presented in Fig. 2. Porosity P (the volume content of pores) in CFRPs is formed by air inclusions, volatile products, and extra moisture during fabrication [36]. It is known that pores scatter ultrasound very effectively; therefore, porosity will cause additional ultrasonic attenuation in CFRP specimens. Porosity P averaged over the entire specimen volume is determined as:

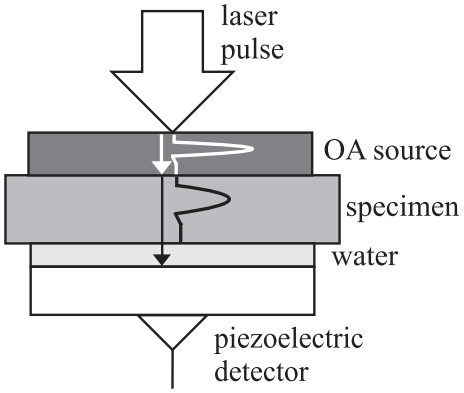

Fig. 1. Diagram of the opto-acoustic cell used in the broadband laser-ultrasonic spectrometer.

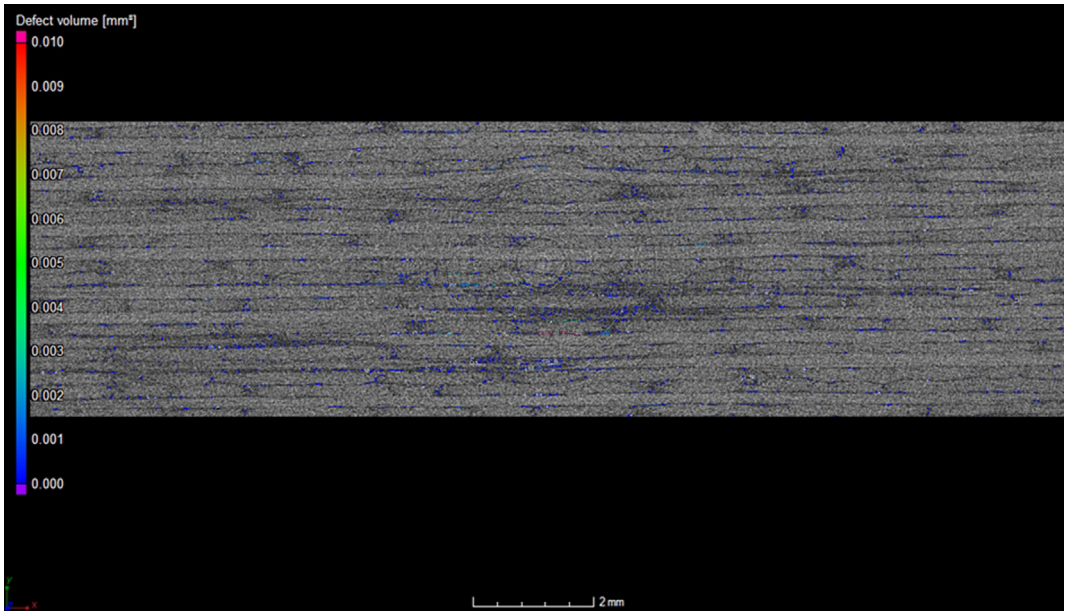

Fig. 2. Example of the X-ray tomography image of the cross-section of composite specimen #4.

$$P = \left(1 - \frac{\rho}{\rho_0}\right) \times 100\%, \tag{9}$$

where actual specimen density ρ is measured using hydrostatic weighing in distilled water (Archimedes' principle); density ρ_0 of the specimen's solid phase or a pore-free composite is calculated using the rule of mixtures with the known densities of the epoxy matrix and carbon fibers, $\rho_m = 1210\,\mathrm{kg/m^3}$, and $\rho_f = 1740\,\mathrm{kg/m^3}$, and their volume contents in the given specimen, n_m and n_f:

$$\rho_0 = n_m\rho_m + n_f\rho_f. \tag{10}$$

The specimens under study differed from each other by the volume content of the epoxy matrix, fibers, and porosity. The technological parameters of all CFRP specimens are summarized in Table 1. The epoxy matrix specimen had the same lateral dimensions as composites, but its thickness was $H_0 = (6.1 \pm 0.06)$ mm.

3.2. Broadband laser-ultrasonic spectroscopy technique

In this work, we use a broadband acoustic spectrometer with laser excitation and piezoelectric detection of ultrasound, which includes a Q-switched Nd:YAG laser operating at the fundamental wavelength (1064 nm), an opto-acoustic (OA) cell, two-channel digital oscilloscope, and PC. The block diagram of the OA cell is shown in Fig. 1. The temporal profile of laser pulses is close to the Gaussian one with the characteristic laser pulse duration of 10–11 ns, the maximum energy is 10 mJ, the pulse repetition rate is 10 Hz, and the characteristic beam diameter is 5 mm.

The absorption of a laser pulse in a special source of sound (OA source) causes nonuniform nonstationary heating and subsequent thermal expansion of its subsurface layer, resulting in the mechanical stress in this layer, which in turn is the origin of longitudinal acoustic waves. A broadband ultrasonic pulse excited in the OA source serves as a reference signal in this spectrometer. In this work, an aqueous solution of Indian black ink was used as the OA source, which was directly placed at a studied specimen. This excluded necessity of using an immersion layer between the OA source and specimen. For the typical CFRP materials with the porosity of about 1–2% the ultrasonic attenuation coefficient varies approximately from 1 to 6 $\mathrm{cm^{-1}}$ in the range of 1–10 MHz (see, for example, [23]). Therefore, the ink concentration in the solution was selected in such a way to provide effective laser excitation of reference ultrasonic pulses in a frequency range up to approximately 15 MHz at the $1/e$ level [25]. This makes it possible to perform reliable measurements of ultrasonic characteristics in our CFRP specimens with the given thicknesses of 10.4–12.4 mm.

The heating of the OA cell under the laser-pulse action is determined by the maximum heating of the subsurface layer of the aqueous solution of ink (OA source) by absorption of these pulses. The light absorption coefficient in this solution at the wavelength of 1064 nm measured by the laser opto-acoustic method [25] was 450 $\mathrm{cm^{-1}}$. The estimation of the corresponding maximum heating of the OA source under a single laser-pulse action using expression (1.10) in [25] gives $T' \approx 6 \times 10^{-4}$ K. To obtain spectra of all ultrasonic pulses, signal averaging over 128 time realizations (128 laser pulses) is carried out, and therefore, the total heating of the OA source during one measurement run is estimated at a level of 0.1 K. This estimation is reliable, since the aqueous solution of ink can be considered as a thermally nonconductive medium (we set its thermal diffusivity equal to that for water $\chi = 1.4 \times 10^{-3}\,\mathrm{cm^2/s}$ [37]). In addition, it can be suggested that during the averaging time (12.8 s), excessive heat does not propagate outward the OA source and other components of the OA cell including a composite specimen remain practically non-heated. Therefore, we consider that all measurements are performed at room temperature.

Broadband ultrasonic pulses are received by a specially designed well-damped piezoelectric 30-μm-thick PVDF-film detector. The resonance frequency of the film is about 28 MHz, but damping makes it possible to provide a quite flat amplitude-frequency response in a frequency range below the resonance. The detector is assembled with a charge preamplifier and operates in an open-circuit mode. The maximum low-frequency sensitivity of this assembly is 2.8 V/bar, its operational bandwidth is 0.5–25 MHz at the $1/e$ level. The calibration procedure of the detector is described in detail in [38]. The acoustic

Table 1
Technological parameters of studied CFRP specimens.

Specimen #	Thickness, mm	Volume content of carbon fibers n_f, %	Porosity P, %
1	10.8 ± 0.1	62.6	< 0.1
2	10.4 ± 0.1	65.1	< 0.1
3	10.7 ± 0.1	62.6	0.7
4	12.4 ± 0.1	55.8	1.4

contact between the specimen and detector in the OA cell is provided by a 3-mm-thick immersion layer of distilled water. In general, the proposed system is similar to any conventional through-transmission spectroscopy setup except for the laser-induced powerful and broadband reference ultrasonic pulses.

Amplitude spectrum of an ultrasonic pulse passed through a studied specimen is:

$$S(f) = S_0(f)T_1T_2\exp[-\alpha(f)H] = S_0(f)T_{\text{trans}}\exp[-\alpha(f)H], \quad (11)$$

where $S_0(f)$ is the amplitude spectrum of the reference pulse, $T_1 = 2Z_s/(Z_s + Z_{\text{ink}})$ is the amplitude coefficient of wave transmission from the OA source (ink) into the composite specimen, $T_2 = 2Z_{H_2O}/(Z_s + Z_{H_2O})T_1 = 2Z_s/(Z_s + Z_{\text{ink}})$ is the amplitude coefficient of wave transmission from the specimen into water, $T_2 = 2Z_{H_2O}/(Z_s + Z_{H_2O})$ Z_sZ_s, Z_{ink}, and Z_{H_2O} are acoustic impedances of the composite specimen, ink, and water, respectively, and $\alpha(f)$ is the frequency-dependent attenuation coefficient of longitudinal acoustic waves in the specimen. From (11), $\alpha(f)$ is expressed as

$$\alpha(f) = \frac{1}{H}\ln\frac{S_0(f)}{S(f)} + \frac{1}{H}\ln T_{\text{trans}}. \quad (12)$$

The acoustic impedance of water at room temperature was considered to be known: $Z_{H_2O} = 1.49 \times 10^6$ kg/(m^{2}s) [37], the acoustic impedances of composite specimens were calculated using experimentally measured densities ρ and the mean phase velocities C of longitudinal acoustic waves in specimens: $Z_s = \rho C$.

Dispersion of the phase velocity of longitudinal acoustic waves, $C(f)$, is calculated using the phase spectrum of the reference ultrasonic pulse, $\phi_0(f)$, and that of the pulse passed through the specimen, $\phi(f)$:

$$C(f) = \frac{2\pi fH}{\phi(f) - \phi_0(f)}. \quad (13)$$

Here, both $\phi_0(f)$ and $\phi(f)$ are already continuous phase spectra obtained using the standard phase unwrapping code [23,39], in which corresponding addition of term $\pm 2\pi n$ (n is an integer) is programmed in such a way to eliminate the ambiguity of the phase spectrum calculated from the arctangent function. For the calculation of $\phi_0(f)$ and $\phi(f)$ using the recorded time profiles of both pulses, oscilloscope triggering starts at the instant of laser pulse emission [38]. For each ultrasonic pulse (reference or passed through a specimen), the time scale of the oscilloscope (horizontal position) is shifted in such a way, that this pulse is displayed on the oscilloscope screen. An example of time profiles of these two ultrasonic pulses is presented in Fig. 3; the actual running time is plotted along the X axis.

Before the attenuation coefficient and velocity dispersion were calculated the correction of the frequency-dependent diffraction loss

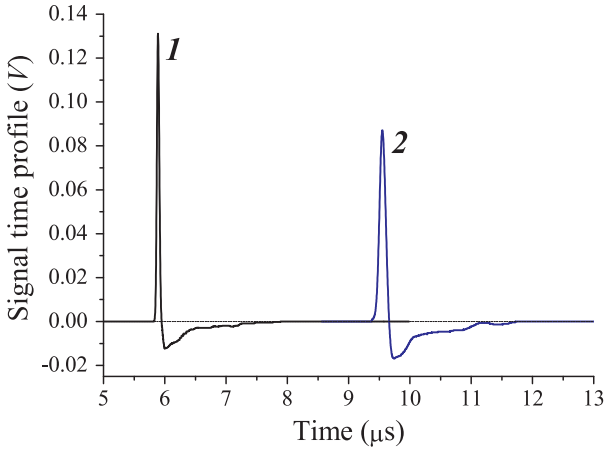

Fig. 3. Examples of the time-domain profiles: (1) the reference ultrasonic pulse and (2) the pulse passed through composite specimen #1.

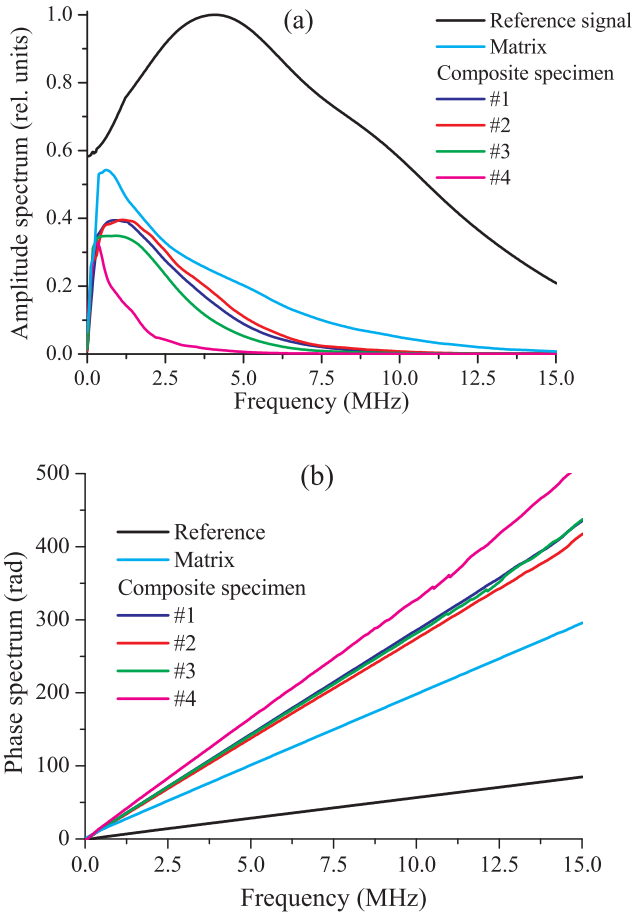

Fig. 4. (a) Amplitude and (b) phase spectra of the reference ultrasonic pulse laser-excited in the aqueous ink solution and of the pulses passed through the epoxy matrix and composite specimens.

was made applying the expressions that describes the diffraction transformation of broadband ultrasonic pulses (see expression (2.47) in [25]).

4. Results and discussion

Fig. 4 shows the amplitude (Fig. 4a) and phase (Fig. 4b) spectra of the reference ultrasonic pulse and that passed through the "pure" epoxy matrix without any filler and through studied CFRP specimens. Clearly, the reference-pulse amplitude spectrum is considerably wider than spectra of pulses passed through all specimens. This confirms the possibility of reliable measurements of ultrasonic attenuation in the studied specimens at least up to 15 MHz. The absence of noise practically up to 15 MHz in the reference phase spectrum provides the same possibility for the phase-velocity measurements.

To analyze the influence of different mechanisms of losses on the relationship between the frequency-dependent attenuation coefficient and phase velocity of longitudinal ultrasonic waves, we studied both specimens of the "pure" epoxy matrix and CFRPs with various porosity. These ultrasonic parameters were calculated using formulas (11) and (12) with the measured amplitude and phase spectra. The dependences $\alpha(f)$ and $C(f)$ in all specimens were obtained in the frequency range of 1–10 MHz. For frequencies $f < 1$ MHz, the attenuation coefficient was not determined because of both its low value and large relative errors caused by diffraction of low-frequency harmonics of a signal in the specimens. For frequencies $f > 10$ MHz, it was also not determined, since signals passed through studied specimens were rather small as compared with the noise level because of considerable ultrasonic

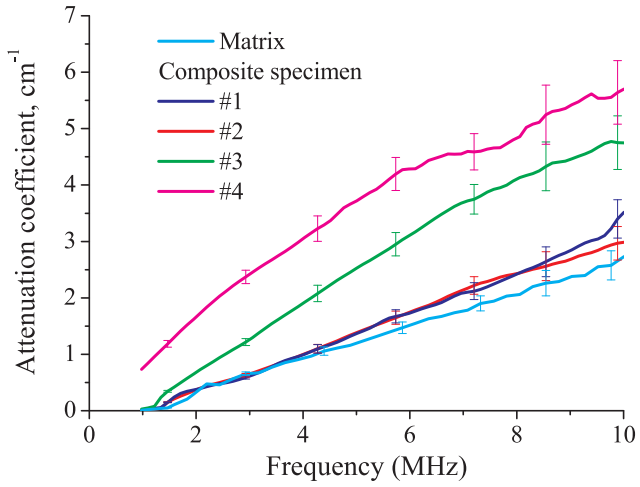

Fig. 5. Frequency dependences of the attenuation coefficient of longitudinal acoustic waves in the epoxy matrix and composite specimens.

attenuation in the specimens. The relative errors of α within the frequency range of 1–10 MHz depend on the signal-to-noise ratio for spectral amplitudes at each harmonic, on the stability of the laser pulse energy, as well as on the measurement uncertainty in the specimen's thickness. These errors change from 5% for the maximum spectral amplitudes to 10% for the minimum spectral amplitudes of ultrasonic signals passed through the specimen. The relative errors of C depend on the same parameters except for the stability of the laser-pulse energy and are estimated at the level of 1–2% within this frequency band.

The frequency dependences of the attenuation coefficient in the epoxy matrix and CFRP specimens are shown in Fig. 5. In pore-free specimens #1 and #2, attenuation is determined by absorption in the matrix and scattering on carbon fibers. In specimens #3 and #4, absolute attenuation increases as compared with specimens 1 and 2 due to the presence of porosity. Here, several uncertainty bounds are shown, which correspond to the minimum and maximum errors for $\alpha(f)$ as described above. The fabrication technology of the studied CFRP specimens yields close acoustic impedances of the matrix and fiber layers and quite high adhesion of fibers to the matrix. Therefore, the reflection of ultrasound at each interface between alternating epoxy and carbon-fiber layers is very weak and attenuation resonances in the studied CFRP specimens are not observed in pore-free specimens #1 and #2. For low-porous specimens #3 and #4, $\alpha(f)$ increases as a whole as compared with the pore-free specimens because of scattering of ultrasound by pores. But the attenuation coefficient also has no resonances, since pores are quite irregularly distributed in the epoxy layers between carbon-fiber plies, the entire porosity is rather small, and therefore no significant decrease in the effective acoustic impedance of the matrix takes place.

To verify applicability of the local Kramers-Kronig relations in the range of 1–10 MHz for all specimens under study, we calculated the phase velocity dispersion using local relation (8), in which we inserted under the integral the experimentally obtained $\alpha(f)$ and the measured velocity at 1 MHz as C_0. We believe that since these relations are linear, for our main purpose it is enough without making additional calculation of the attenuation coefficient using the experimentally measured phase-velocity dispersion. Fig. 6 shows the calculated velocity together with the experimentally measured dependence $C(f)$ for the matrix. Here, also several typical uncertainty bound are shown, which correspond to the minimum and maximum errors for $C(f)$. Clearly, in the studied frequency range 1–10 MHz, the experimental and calculated dependences coincide within the limits of the measurement accuracy. However, some deviations of the calculated curve from the experimentally obtained phase velocity in the low- and high-frequency range are observed. These deviations are because of the value of C_0 used to

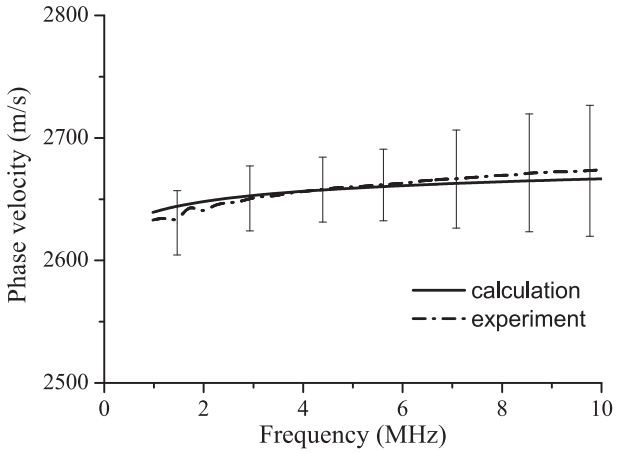

Fig. 6. Frequency dependence of the phase velocity of longitudinal acoustic waves in the epoxy matrix specimen.

obtain calculated dependence $C(f)$ is also measured with an error of 1–2% and also because of calculation formula (8) provides certainly not the actual velocities at each frequency, but their approximate values within the framework of the assumptions made by deriving this formula (Section 2). Hence, for the epoxy matrix, applicability of local Kramers-Kronig relations was confirmed. In the matrix, the relative phase velocity dispersion of longitudinal acoustic waves is $\Delta C = \frac{C_{max} - C_{min}}{C_{max}} \times 100\% \approx 17\%$ (where C_{max} and C_{min} are the maximum and minimum velocity values in the range of 1–10 MHz) and is determined by peculiarities of the epoxy molecular structure. This dispersion could be explained by relaxation processes occurring as a result of different molecular motions. If an ultrasonic frequency is low and corresponding period is high as compared with a relaxation time for the largest macromolecule segments, the energy of the ultrasonic wave obtained over a period by an elementary volume will rapidly redistribute over the material volume due to segmental mobility of macromolecules [35]. By the increase in the ultrasonic frequency, the time of absorption will take a most part of the period. In this case, there are some segments, which are not able to transmit the wave energy to the neighbor segments during one oscillation period. In other words, under the external wave impact they behave as rigid elements of molecular chains. This leads to the increase in the ultrasonic velocity by the increase in the frequency.

Figs. 7 and 8 present similar calculated and experimental

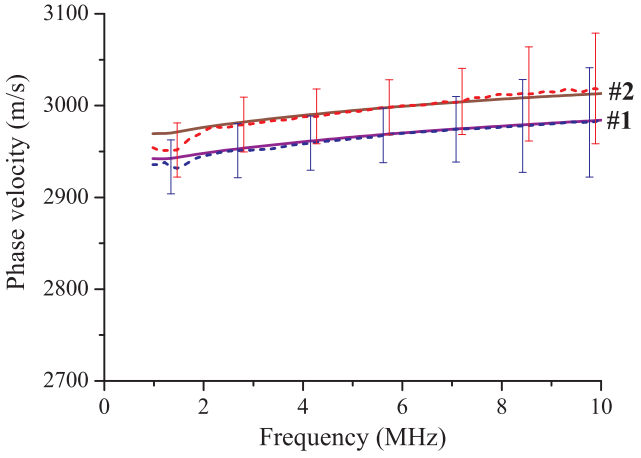

Fig. 7. Experimental and calculated frequency dependences of the phase velocity of longitudinal acoustic waves in pore-free composite specimens #1 and #2. Dotted curves are the experimental results; solid curves are the calculation results obtained with expression (8).

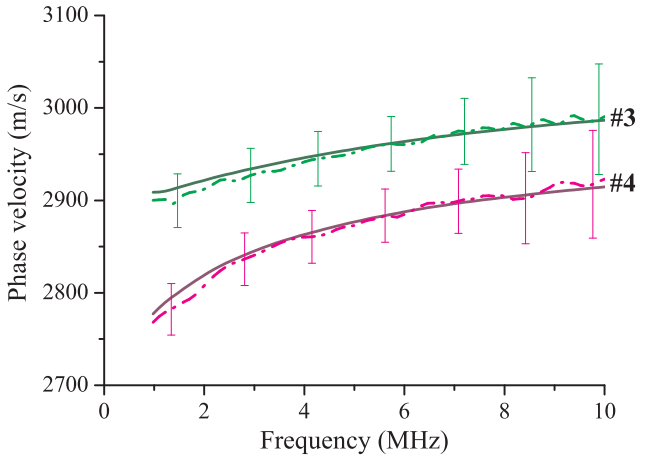

Fig. 8. Frequency dependences of the phase velocity of longitudinal acoustic waves in low-porous composite specimens #3 and #4. Dotted curves are the experimental results; solid curves are the calculation results obtained with expression (8).

dependences $C(f)$ for the studied CFRP specimens. Just as for the epoxy matrix, several typical uncertainty bound are shown, which correspond to the minimum and maximum errors for $C(f)$. Clearly, in the operating frequency range of 1–10 MHz, the calculated and measured dependences $C(f)$ coincide within the limits of the measurement accuracy. Therefore, applicability of the local Kramers-Kronig relations is also confirmed for CFRPs independent of a physical reason of ultrasonic wave attenuation.

As it was mentioned above, in pore-free CFRP specimens #1 and #2, both the ultrasonic velocity dispersion and absolute attenuation in the entire operating frequency range are determined by absorption in the matrix and scattering on carbon fibers. The porosity in composite specimens #3 and #4 leads to additional scattering by pores and to the observed increase of the relative dispersion of the ultrasonic velocity. For specimen #3 $\Delta C \approx 30\%$ at $P = 0.7\%$ and for specimen #4 $\Delta C \approx 45\%$ at $P = 1.4\%$, whereas for pore-free composites $\Delta C \approx 20\%$ in the same spectral range. Therefore, for the most porous CFRP specimen, the relative dispersion increases more than twice as compared with pore-free specimens. It should be noted that in the operating frequency range, the increase of value C_{max} was observed with the increase of the volume content of carbon fibers in the specimen, since the ultrasonic velocity in fibers is higher than that in the matrix. Figs. 7 and 8 show that for specimens #1 and #3 with the same fiber content (62.6%), C_{max} coincides within the limits of accuracy and is 2985 ± 15 m/s. For specimen #2 with the maximum fiber content (65.1%) $C_{max} \approx 3017 \pm 15$ m/s and for specimen #4 with the minimum fiber content (55.8%) $C_{max} \approx 2917 \pm 15$ m/s. At the same time, minimum velocity C_{min} demonstrates decreasing with the increase of the specimen porosity independent of the fiber content. Such combined behavior of C_{max} and C_{min} leads to the increase in the relative phase-velocity dispersion with the increase of the composite porosity. The low-frequency dispersion of the ultrasonic velocity was theoretically analyzed in [40] using the mathematical analogy between plane wave propagation through a material with voids and axial wave propagation along a circular cylindrical rod with radial shear and inertia. In a rod, an ultrasonic pulse begins to propagate with the maximum longitudinal velocity and when due to the radial shear strain its energy is transformed into a dispersive wave, which propagates with a lower bar velocity. In a porous material, similar transformation occurs due to dilatational inertia around voids. The velocity of this dispersive wave is determined by a bulk elastic modulus and is less than the velocity of longitudinal waves in the pore-free material. The efficiency of such transformation and corresponding strength of the dispersive effect depend on the ratio of characteristic scales of the corresponding process, for example, of a rod diameter or pore sizes and ultrasonic frequencies.

It should be especially noted that the obtained results in a part of the relationship between ultrasonic attenuation and the phase velocity via the local Kramers-Kronig relations are solely presented to confirm the fundamental physical principles of causality and linearity, since these relations are just the mathematical representation of these principles. The results are obtained using the experimental data, are attributed to particular CFRP composites and do not pretend to obtain on its basis a "unified" general relation between attenuation and velocity after approximation by some power-law functions [4,12–14] or by application of a modern sophisticated neural network algorithm, as it was made, for example in [34]. In addition, we have shown that the proposed broadband laser-ultrasonic spectroscopy method makes it possible to measure both attenuation and velocity of ultrasound with a high accuracy enough for ultrasonic nondestructive evaluation or defect image reconstruction. These measurements can be carried out for materials, which generally could not obey a single power-law with the same index in the entire studied frequency range. Such materials are, for instance, polycrystalline metals with a wide grain-size distribution (see, for example [41]), or metal-matrix composites reinforced with disperse high-strength ceramic particles, which strongly differ in size and shape.

5. Conclusions

In this work, we analyzed the local Kramers-Kronig relations for the attenuation coefficient and phase velocity in CFRPs in the frequency range of 1–10 MHz. Verification of these relations was experimentally performed using the broadband acoustic spectroscopy method with the laser source of ultrasound. This method makes it possible to measure the frequency dependences of the attenuation coefficient and phase velocity of longitudinal ultrasonic waves in the megahertz range for intensely ultrasound- absorbing and scattering materials. By the example of the "pure" epoxy matrix without any filler and epoxy-based CFRPs, we have analyzed influence of two mechanisms of losses of the acoustic energy, i.e., absorbing and scattering, on ultrasonic attenuation and velocity dispersion. In the matrix, attenuation and dispersion are caused by absorption of ultrasound due to relaxation processes occurring in the ultrasonic-wave field. In CFRPs, scattering on carbon fibers and gas pores of several tenths of microns in size additionally contributes to attenuation and dispersion of ultrasonic waves. We have shown experimentally that in the frequency range of 1–10 MHz, the maximum absolute value of the phase velocity is higher for the larger volume content of carbon fibers. At the same time, the increase in porosity leads to the increase in relative phase-velocity dispersion independent on the volume content of the CFPR components.

To verify applicability of the local Kramers-Kronig relations, we have calculated dispersion of the phase velocity using the experimentally measured frequency dependences of the attenuation coefficient of longitudinal acoustic waves. Then, we have compared the calculation results with experimentally measured dispersion of the phase velocity. Coincidence within the limits of the measurement accuracy of the calculated and experimentally obtained frequency dependences of the phase velocity for the studied frequency range of 1–10 MHz confirms applicability of the approximate local form of the local Kramers-Kronig relations both for the epoxy matrix and all studied CFRP specimens. Therefore, these dispersion relations are applicable independent of a particular mechanism of losses in the energy of ultrasonic waves by propagation in the studied materials.

CRediT authorship contribution statement

Yu.G. Sokolovskaya: Formal analysis, Investigation, Writing - original draft, Visualization. **N.B. Podymova:** Conceptualization, Methodology, Investigation, Writing - review & editing. **A.A. Karabutov:** Supervision.

References

[1] L.D. Landau, E.M. Lifshitz, Electrodynamics of Continuous Media, Pergamon Press, 1984.
[2] V.L. Ginzburg, On the general relationship between the absorption and dispersion of sound waves, Sov. Phys. Acoust. 1 (1955) 31–39.
[3] M. O'Donnell, E.T. Jaynes, J.G. Miller, General relationships between ultrasonic attenuation and dispersion, J. Acoust. Soc. Am. 63 (1978) 1935–1937.
[4] T.L. Szabo, Causal theories and data for acoustic attenuation obeying a frequency power law, J. Acoust. Soc. Am. 97 (1995) 14–24.
[5] M. O'Donnell, E.T. Jaynes, J.G. Miller, Kramers-Kronig relationship between ultrasonic attenuation and phase velocity, J. Acoust. Soc. Am. 69 (1981) 696–701.
[6] J. Mobley, K.R. Waters, J.G. Miller, Finite-bandwith effects on the causal prediction of ultrasonic attenuation of the power-law form, J. Acoust. Soc. Am. 114 (2003) 2782–2790.
[7] D.W. Fitting, L. Adler, Ultrasonic Spectral Analysis for Nondestructive Evaluation, Plenum Press, New York, 1981.
[8] A. Vary, Material property characterization, in: P.O. Moore (Ed.), Nondestructive Testing Handbook. Ultrasonic Testing, ASTM, Columbus, 2007.
[9] T. Inoue, T. Norisuye, K. Sugita, H. Nakanishi, Q. Tran-Cong-Miyata, Size distribution and elastic properties of thermo-responsive polymer gel microparticles in suspension probed by ultrasonic spectroscopy, Ultrasonics 82 (2018) 31–38.
[10] H. Mori, T. Norisuye, H. Nakanishi, Q. Tran-Cong-Miyata, Ultrasound attenuation and phase velocity of micrometer-sized particle suspensions with viscous and thermal losses, Ultrasonics 83 (2018) 171–178.
[11] J. Wu, Determination of velocity and attenuation of shear waves using ultrasonic spectroscopy, J. Acoust. Soc. Am. 99 (1996) 2871–2875.
[12] T.L. Szabo, J. Wu, A model for longitudinal and shear wave propagation in viscoelastic media, J. Acoust. Soc. Am. 107 (2000) 2437–2446.
[13] F. Mainardi, Fractional Calculus and Waves in Linear Viscoelasticity, first ed., Imperial College Press, London, 2010, pp. 77–107.
[14] S. Holm, S.P. Näsholm, A causal and fractional all-frequency wave equation for lossy media, J. Acoust. Soc. Am. 130 (2011) 2195–2202.
[15] R. Truell, C. Elbaum, B. Chick, Ultrasonic Methods in Solid State Physics, Academic Press, New York, 1969.
[16] D. Zellouf, Y. Jayet, N. Saint Pierre, J. Tatibouët, J.C. Baboux, Ultrasonic spectroscopy in polymeric materials. Application of the Kramers-Kronig relations, J. Appl. Phys. 80 (1996) 2728–2732.
[17] E.L. Carstensen, K. Li, H.P. Schwan, Determination of the acoustic properties of blood and its components, J. Acoust. Soc. Am. 25 (1953) 286–289.
[18] K. Füzesi, N. Ilyina, E. Verboven, K. Abeele Van Den, M. Gyöngy, J. D'hooge, Temperature dependence of speed of sound and attenuation of porcine left ventricular myocardium, Ultrasonics 82 (2018) 246–251.
[19] E.L. Carstensen, Relaxation processes in aqueous solutions of $MnSO_4$ and $CoSO_4$, J. Acoust. Soc. Am. 26 (1954) 862–864.
[20] K.R. Waters, M.S. Hughes, J. Mobley, G.H. Brandenburger, J.G. Miller, On the applicability of Kramers-Kronig relations for ultrasonic attenuation obeying a frequency power law, J. Acoust. Soc. Am. 108 (2000) 556–563.
[21] R.L. Trousil, K.R. Waters, J.G. Miller, Experimental validation of the use of Kramers-Kronig relations to eliminate the phase sheet ambiguity in broadband phase spectroscopy, J. Acoust. Soc. Am. 109 (2001) 2236–2244.
[22] F.J. Alvarez, R. Kuc, Dispersion relation for air via Kramers-Kronig analysis, J. Acoust. Soc. Am. 124 (2008) 57–61.
[23] H. Jeong, D.K. Hsu, Experimental analysis of porosity-induced ultrasonic attenuation and velocity change in carbon composites, Ultrasonics 33 (1995) 195–203.
[24] C.B. Scruby, L.E. Drain, Laser Ultrasonics: Techniques and Applications, Adam Hilger, Bristol, 1990.
[25] V.E. Gusev, A.A. Karabutov, Laser Optoacoustics, American Institute of Physics, New York, 1993.
[26] D.E. Chimenti, Review of air-coupled ultrasonic materials characterization, Ultrasonics 54 (2014) 1804–1816.
[27] B. Hutchinson, P. Lundin, E. Lindh-Ulmgren, D. Lévesque, Anomalous ultrasonic attenuation in ferritic steels at elevated temperatures, Ultrasonics 69 (2016) 268–272.
[28] C.M. Kube, Attenuation of laser generated ultrasound in steel at high temperatures; comparison of theory and experimental measurements, Ultrasonics 70 (2016) 238–240.
[29] J. Laloš, M. Jezeršek, R. Petkovšek, T. Pozar, Laser-induced ultrasonic waveform derivation and transition from a point to a homogeneous illumination of a plate, Ultrasonics 81 (2017) 158–166.
[30] A.A. Karabutov, M.P. Matrosov, N.B. Podymova, V.A. Pyzh, Acoustic pulse spectroscopy using a laser sound source, Sov. Phys. Acoust. 37 (1991) 157–163.
[31] A.A. Karabutov, N.B. Podymova, Nondestructive evaluation of fatigue-induced changes in the structure of composites by a laser ultrasonic method, Mech. Compos. Mater. 31 (1995) 198–203.
[32] A.A. Karabutov, N.B. Podymova, I.O. Belyaev, The influence of porosity on ultrasound attenuation in carbon fiber reinforced plastic composites using the laser-ultrasound spectroscopy, Acoust. Phys. 59 (2013) 667–673.
[33] L.D. Landau, E.M. Lifshitz, Theory of Elasticity, Pergamon Press, 1970.
[34] J.S. Egerton, M.J.S. Lowe, P. Huthwaite, H.V. Halai, Ultrasonic attenuation and phase velocity of high-density polyethylene pipe material, J. Acoust. Soc. Am. 141 (2017) 1535–1545.
[35] I.I. Perepechko, Introduction to Polymer Physics, Mir Publishes, Moscow, 1981.
[36] R.D. Adams, P. Cawley, A review of defect types and nondestructive testing techniques for composites and bonded joints, NDT Int. 21 (1988) 208–222.
[37] Handbook of Physical Quantities, I.S. Grigoriev, E.Z. Meilikhov, A.A. Radzig, (Ed.), CRC-Press, Boca Raton, 1997.
[38] N.B. Podymova, A.A. Karabutov, Broadband laser-ultrasonic spectroscopy for quantitative characterization of porosity effect on acoustic attenuation and phase velocity in CFRP laminates, J. Nondestruct. Eval. 33 (2014) 141–151.
[39] M. Ourak, B. Nongaillard, J.M. Rouvaen, M. Ouaftouh, Ultrasonic spectroscopy of composite materials, NDT Int. 24 (1991) 21–28.
[40] T.W. Wright, Elastic wave propagation through a material with voids, J. Mech. Phys. Solids 46 (1998) 2033–2047.
[41] F.E. Stanke, G.S. Kino, A unified theory for elastic wave propagation in polycrystalline materials, J. Acoust. Soc. Am. 75 (1984) 665–681.